symmetry

MDPI

Article

Timelike Surface Couple with Bertrand Couple as Joint Geodesic Curves in Minkowski 3-Space

Fatemah Mofarreh

Mathematical Science Department, Faculty of Sciences, Princess Nourah Bint Abdulrahman, Riyadh 11546, Saudi Arabia; fyalmofarrah@pnu.edu.sa

Abstract: A curve on a surface is a geodesic curve if its principal normal vector is anywhere aligned with the surface normal. Using the Serret–Frenet frame, a timelike surface couple ($\mathcal{TLSC}$) with the symmetry of a Bertrand couple ($\mathcal{BC}$) can be specified in terms of linear combinations of the components of the local frames in Minkowski 3-space $\mathcal{E}_1^3$. With these parametric representations, the necessary and sufficient conditions for the specified $\mathcal{BC}$ are derived to be the geodesic curves defining these surfaces. Afterward, the definition of a $\mathcal{TL}$ ruled surface ($\mathcal{RS}$) is also provided. Furthermore, the application of the method to some significant models is given.

Keywords: Bertrand couple; isoparametric timelike ruled surface

MSC: 53A04; 53A17; 53B50; 53B30

1. Introduction

In the context of differential geometry, a geodesic along two points on a surface is defined as a curve embedded in the surface with the least distance along the points. In fact, the sufficient and necessary conditions that a curve on a surface is a geodesic is that the rectifying plane of the curve and the surface tangent plan are identical [1,2]. The geodesic also plays a role in the relativistic description of gravity. Einstein's concept of equality says that the geodesic manifests the locus of a freely falling particle in a specified space. (Freely landing in this situation means movable only down the influence of gravity, with no other forces involved). The geodesic concept states that the free locus is the geodesic of space. It plays a fully considerable role in a geometric-relativity theory, since it means that the basic equation of dynamics is fully endowed by the geometry of space and subsequently is not to be set as an independent equation. Furthermore, in such a theory, the attitude is distinguished (up to a stationary) by the major length invariant, so that the stable attitude principal and the geodesic principle become identical [3,4]. Geodesics have been widely applied in different fields, such as cutting and painting paths, tent industrialization, fiberglass tape furls in pipe industrialization, and textile industrialization [5,6]. Is is also used for Fermat's principle in classical optics, and as a cornerstone of general relativity. Normally, the key consideration in geodesic research is how to find and depict geodesics on the considered surfaces, and there are a large number of papers focused on this matter. For example, the studies were carried out for the polymer case to find the shortest distance, as in [7], while it focused more on the directions of the geodesics of physical four-dimensional space–times [8]. Furthermore, other studies examined geodesic curves in various cases such as polynomial surfaces [9], convex polytopes in three dimensions [10,11] or even as applications as in [12–14], where the idea of geodesics applied to a change in sail design, for object segmentation in images and the fast marching method for solving the Eikonal equation on triangular meshes, respectively. Most of the previous work about surface curves focuses on how to find them on a given surface. However, the more relevant problem is to find surfaces passing through a given curve and accepting it as a special curve, such

Citation: Mofarreh, F. Timelike Surface Couple with Bertrand Couple as Joint Geodesic Curves in Minkowski 3-Space. *Symmetry* **2024**, *16*, 732. https://doi.org/10.3390/sym16060732

Academic Editors: Luca Grilli, Süleyman Şenyurt and Marian Ioan Munteanu

Received: 17 February 2024
Revised: 19 March 2024
Accepted: 5 June 2024
Published: 12 June 2024

as a geodesic, asymptotic curve or line of curvature. In [15], Wang et al. investigated the issue of constructing a bundle of surfaces from a delineated geodesic curve for which each surface could be considered a candidate for style planning. They evidenced the necessary and sufficient situation for the coefficients to be significant under both the geodesic and isoparametric requirements. Later, a large number of research efforts dealing with bundles of surfaces having a conjoint distinctive curve in both Euclidean and non-Euclidean spaces. For example, the recent methods are used to construct developable surface depending on a given curve, a given line of curvature or given curve as its common asymptotic curve by applying the parametric representation of the developable surfaces, because this is very important in the field of geometric design and surfaces analysis [16–18]. Moreover, in [19], in Euclidean 3-space, a Smarandache curve that is geodesic and isoparametric is used to find a surfaces family with the use of a Frenet frame, while another study was performed in the same space but with the use of common geodesic curves [20]. On the other hand, R.A. Abdel-Baky [21] presented a study that constructed a timelike surface pencil from a given spacelike or timelike asymptotic curve in Minkowski 3-space. Similar studies into the same kind of the space were performed but in the case of a given spacelike or timelike line of curvature [22]. Recently, a common asymptotic null curve is used to build a surface family, as well as providing the necessary and sufficient conditions for them to be ruled and developable surfaces [23]. In addition, using the Cartan frame, a surfaces family was constructed with an asymptotic curve where the surface was presented as a linear combination of this frame [24,25]. Furthermore, the focus of the concept of a Bertrand pair appears in recent studies more in [26,27], where both studies were carried out in the Galilean space, but the first used a Bertrand pair as common asymptotic curves and the other used a Bertrand pair as common geodesic curves.

In the theory of curves, the conformable interconnection of curves is a perfect issue to be investigated. A Bertrand couple ($\mathcal{BC}$) is one of the classic distinguished curves. Two curves are a $\mathcal{BC}$ if there exists a bijection between them such that both curves have common principal normals [1,2,28]. $\mathcal{BC}$s have been utilized as private models of offset curves in computer-aided design ($\mathcal{CAD}$) and computer-aided manufacture ($\mathcal{CAM}$) (see [29–31]). Different researchers investigated Bertrand curves, which are important for the theory of curves, in different cases with various conditions and spaces, such as in [32–36]. The generalization of Bertrand curves was investigated in [37] with respect to the casual characters of the curves in Minkowski space–time.

Some of the previous studies are related to the topic of this paper but not focused on the same details for both timelike surfaces and geodesic curves, especially in the Minkowski space with the concept of a Bertrand couple. For example, for the timelike surfaces, it is proven that the Gauss map and mean curvature both satisfy a system in the partial differential equations [38]. Another study was performed by Mehmet et al. [39], who gave the Frenet frames as well as Frenet invariants in the case of timelike ruled surfaces in the Minkowski 3-space. Murat et al. [40] investigated time-like loxodromes at rotational surfaces in the Minkowski 3-space, and later, another study presented the kinematic geometry of the timelike ruled surface considering a constant Disteli-axis under special cases such as a one-parameter screw motion in the same space [41]. In [42], differential equations for the space-like loxodromes on helicoidal surfaces in the Minkowski 3-space were calculated by Murat et al. More recently, in Ref. [43], timelike circular surfaces are parameterized, and some geometric properties such as singularities, striction curves, and Gaussian and mean curvatures are examined. Furthermore, in [44], the singularities are classified by the osculating developable surface, in addition to giving a relation between both the osculating Darboux vector fields and normal vector fields of timelike surfaces along the curve using Legendrian dualities. Additionally, in the Lorentz–Minkowski 3-space, the relation between geodesic torsions, normal curvatures and geodesic curvatures for parameter curves that intersect at any angle in case of timelike surfaces are investigated [45]. However, to the best of our knowledge, no work has focused on constructing $\mathcal{TLSC}$ using a $\mathcal{BC}$ as a pair of geodesic curves in the Minkowski 3-space $\mathcal{E}_1^3$. This work proposes to fill this research gap and discusses the use of a $\mathcal{BC}$ as a pair of geodesic curves to construct $\mathcal{TLSC}$ in the Minkowski 3-space $\mathcal{E}_1^3$.

The key contribution of this work is the construction of $\mathcal{TLSC}$ with $\mathcal{BC}$ as geodesic curves in the Minkowski 3-space $\mathcal{E}_1^3$. Then, employing the Serret–Frenet frame, the necessary and sufficient conditions for $\mathcal{TLSC}$ embedding a $\mathcal{BC}$ as joint geodesic curves are determined. Afterward, the definition of $\mathcal{TLRS}$ is also inspected. Furthermore, models are considered to demonstrate the implementation of the theoretical results. This study is purposed to add to the geometric analysis of timelike surface couples through the timelike Bertrand couple.

2. Preliminaries

Let $\mathcal{E}_1^3$ indicate the Minkowski 3-space [3,4]. For the vectors $\mathfrak{u} = (u_1, u_2, u_3)$ and $\mathfrak{v} = (v_1, v_2, v_3)$ in $\mathcal{E}_1^3$,

$$\langle \mathfrak{u}, \mathfrak{v} \rangle = u_1 v_1 - u_2 v_2 + u_3 v_3$$

is called the Lorentzian inner product. The vector is defined as

$$\mathfrak{u} \times \mathfrak{v} = (u_2 v_3 - u_3 v_2, u_1 v_3 - u_3 v_1, u_1 v_2 - u_2 v_1).$$

As $\langle , \rangle$ is an indefinite metric, recall that a vector $\mathfrak{u} \in \mathcal{E}_1^3$ can have one of three causal natures: it can be spacelike ($\mathcal{SL}$) if $\langle \mathfrak{u}, \mathfrak{u} \rangle > 0$ or $\mathfrak{u} = \mathbf{0}$, $\mathcal{TL}$ if $\langle \mathfrak{u}, \mathfrak{u} \rangle < 0$ and lightlike or null if $\langle \mathfrak{u}, \mathfrak{u} \rangle = 0$ and $\mathfrak{u} \neq \mathbf{0}$. The norm of $\mathfrak{u} \in \mathcal{E}_1^3$ is denoted by $\|\mathfrak{u}\| = \sqrt{|\langle \mathfrak{u}, \mathfrak{u} \rangle|}$. Then, the hyperbolic and Lorentzian (de Sitter space) unit spheres are defined as

$$\mathcal{H}_+^2 = \{\mathfrak{u} \in \mathcal{E}_1^3 \mid \|\mathfrak{u}\|^2 := u_1^2 - u_2^2 + u_3^2 = -1, u_1 > 0\}, \tag{1}$$

and

$$\mathcal{S}_1^2 = \{\mathfrak{u} \in \mathcal{E}_1^3 \mid \|\mathfrak{u}\|^2 := u_1^2 - u_2^2 + u_3^2 = 1\}. \tag{2}$$

Let $\boldsymbol{\omega}(v)$ be a unit-speed $\mathcal{TL}$ curve in $\mathcal{E}_1^3$ and suppose, without loss of generality, that $\boldsymbol{\omega}$ is represented by the arc-length parameter $v \in I \subseteq \mathbb{R}$. If $\{\varsigma_1(v), \varsigma_2(v), \varsigma_3(v)\}$ is the Serret–Frenet frame ($\mathcal{SF}$) along $\boldsymbol{\omega}(v)$, then the $\mathcal{SF}$ formulae read:

$$\begin{pmatrix} \varsigma_1' \\ \varsigma_2' \\ \varsigma_3' \end{pmatrix} = \begin{pmatrix} 0 & \kappa(v) & 0 \\ \kappa(v) & 0 & \tau(v) \\ 0 & -\tau(v) & 0 \end{pmatrix} \begin{pmatrix} \varsigma_1 \\ \varsigma_2 \\ \varsigma_3 \end{pmatrix}, \tag{3}$$

where $\kappa(v)$ and $\tau(v)$ denote the curvature and torsion of $\boldsymbol{\omega}(v)$, respectively. One can also show that

$$\begin{gathered} -\langle \varsigma_1, \varsigma_1 \rangle = \langle \varsigma_2, \varsigma_2 \rangle = \langle \varsigma_3, \varsigma_3 \rangle = 1, \\ \varsigma_1 \times \varsigma_2 = \varsigma_3, \ \varsigma_1 \times \varsigma_3 = -\varsigma_2, \ \varsigma_2 \times \varsigma_3 = -\varsigma_1. \end{gathered} \tag{4}$$

The subspaces $Sp\{\varsigma_1, \varsigma_2\}$, $Sp\{\varsigma_2, \varsigma_3\}$and $Sp\{\varsigma_3, \varsigma_1\}$ are named the osculating plane, normal plane and rectifying plane, respectively. Similarly, in line with [1,2], the following definition is given:

Definition 1. *Two $\mathcal{TL}$ curves $\boldsymbol{\omega}(v)$ and $\widehat{\boldsymbol{\omega}}(v)$ are $\mathcal{BC}$ if there exists a bijection among them such that they have a common principal normal, and*

$$\widehat{\boldsymbol{\omega}}(v) = \boldsymbol{\omega}(v) + f\varsigma_2(v), \tag{5}$$

where f is a stationary .

A surface $\mathcal{M}$ is defined by

$$\mathcal{M} : \mathfrak{r}(v,t) = (\mathfrak{r}_1(v,t), \mathfrak{r}_2(v,t), \mathfrak{r}_3(v,t)), \ \ (v,t) \in \mathbb{D} \subseteq \mathbb{R}^2. \tag{6}$$

If $\mathfrak{r}_v(v,t) = \frac{\partial \mathfrak{r}}{\partial v}$ *and* $\mathfrak{r}_t(v,t) = \frac{\partial \mathfrak{r}}{\partial t}$, *then the surface normal is*

$$\mathcal{N}(v,t) = \mathfrak{r}_v \wedge \mathfrak{r}_t, \ \langle \mathcal{N}, \mathfrak{r}_v \rangle = \langle \mathcal{N}, \mathfrak{r}_t \rangle = 0. \tag{7}$$

A curve on a surface is geodesic if and only if the normal vector to the curve is everywhere parallel to the local normal vector of the surface [1,2].

A surface in $\mathcal{E}_1^3$ is called a $\mathcal{TL}$ surface if the induced metric on the surface is a Lorentzian metric and is called a $\mathcal{SL}$ surface if the induced metric on the surface is a positive definite Riemannian metric; that is, the surface normal is a $\mathcal{TL}$ ($\mathcal{SL}$) vector [3,4].

An isoparametric curve $\boldsymbol{\omega}(v)$ is a curve on a surface $\mathcal{M} : \mathfrak{r}(v,t)$ in $\mathcal{E}_1^3$ that has a constant v or t-parameter value. In other words, there exists a parameter t_0 or v_0 such that $\boldsymbol{\omega}(v) = \mathfrak{r}(v, t_0)$ or $\boldsymbol{\omega}(t) = \mathfrak{r}(v_0, t)$. Given a parametric curve $\boldsymbol{\omega}(v)$, it is clear that $\boldsymbol{\omega}(v)$ is an isogeodesic of $\mathcal{M} : \mathfrak{r}(v,t)$ if it is both a geodesic and an isoparametric curve on $\mathcal{M} : \mathfrak{r}(v,t)$.

3. Main Results

This section presents a novel method for construction of a $\mathcal{TLSC}$ with a $\mathcal{BC}$ as a pair of common geodesic curves in $\mathcal{E}_1^3$. For this purpose, consider a $\mathcal{TLBC}$ such that the tangent planes of the $\mathcal{TLSC}$ are simultaneous with the rectifying planes of the $\mathcal{TLBC}$.

Consider that $\boldsymbol{\omega}(v)$ and $\widehat{\boldsymbol{\omega}}(v)$ are two $\mathcal{TLBC}$. If $\{\kappa(v), \tau(v), \varsigma_1(v), \varsigma_2(v), \varsigma_3(v)\}$ and $\{\widehat{\kappa}(v), \widehat{\tau}(v), \widehat{\varsigma}_1(v), \widehat{\varsigma}_2(v), \widehat{\varsigma}_3(v)\}$ are two Frenet–Serret frames of $\boldsymbol{\omega}(v)$ and $\widehat{\boldsymbol{\omega}}(v)$, respectively, then

$$\mathcal{M} : \mathfrak{r}(v,t) = \boldsymbol{\omega}(v) + \mathfrak{x}(v,t)\varsigma_1(v) + \mathfrak{y}(v,t)\varsigma_3(v); \ 0 \le t \le T, \ 0 \le v \le L \tag{8}$$

is a $\mathcal{TL}$ surface bundle $\mathcal{M}$ with $\boldsymbol{\omega}(v)$ as a joint curve. Similarly, the $\mathcal{TL}$ surface bundle $\widehat{\mathcal{M}}$ along $\widehat{\boldsymbol{\omega}}(v)$ is

$$\widehat{\mathcal{M}} : \widehat{\mathfrak{r}}(v,t) = \widehat{\boldsymbol{\omega}}(v) + \mathfrak{x}(v,t)\widehat{\varsigma}_1(v) + \mathfrak{y}(v,t)\widehat{\varsigma}_3(v); \ \ 0 \le t \le T, \ 0 \le v \le L, \tag{9}$$

where $\mathfrak{x}(v,t), \mathfrak{y}(v,t) \in C^1$ are called marching-scale functions and are differentiable functions at least of order 1, with the constraint $\mathfrak{y}(v,t_0) \neq 0$.

For $\widehat{\mathcal{M}}$ with $\widehat{\boldsymbol{\omega}}(v)$ as a joint geodesic $\mathcal{TL}$ curve, according to Equation (9), it is expected that the marching-scale functions should be satisfied . Simplifying the calculations, we have

$$\left.\begin{array}{l} \widehat{\mathfrak{r}}_v(v,t) = (1+\mathfrak{x}_v)\widehat{\varsigma}_1 + (\mathfrak{x}\widehat{\kappa} + \widehat{\tau}\mathfrak{y})\widehat{\varsigma}_2 + \mathfrak{y}_s\widehat{\varsigma}_3, \\ \widehat{\mathfrak{r}}_t(v,t) = \mathfrak{x}_t\widehat{\varsigma}_1 + \mathfrak{y}_t\widehat{\varsigma}_3, \end{array}\right\} \tag{10}$$

and

$$\widehat{\mathcal{N}}(v,t) := \widehat{\mathfrak{r}}_v \times \widehat{\mathfrak{r}}_t = (\mathfrak{x}\widehat{\kappa} + \mathfrak{y}\widehat{\tau})\mathfrak{y}_t\widehat{\varsigma}_1 + [(1+\mathfrak{x}_v)\mathfrak{y}_t - \mathfrak{y}_v\mathfrak{x}_t]\widehat{\varsigma}_2 - (\mathfrak{x}\widehat{\kappa} + \mathfrak{y}\widehat{\tau})\mathfrak{x}_t\widehat{\varsigma}_3. \tag{11}$$

As $\widehat{\boldsymbol{\omega}}(v)$ is an isoparametric on $\widehat{\mathcal{M}}$, there exists a value $t_0 \in [0,T]$ such that $\widehat{\mathfrak{r}}(v,t_0) = \widehat{\boldsymbol{\omega}}(v)$; that is,

$$\mathfrak{x}(v,t_0) = \mathfrak{y}(v,t_0) = 0, \ \mathfrak{x}_v(v,t_0) = \mathfrak{y}_v(v,t_0) = 0. \tag{12}$$

Thus, when $t = t_0$, that is, on $\widehat{\boldsymbol{\omega}}(v)$, we have

$$\widehat{\mathcal{N}}(v,t_0) = \mathfrak{y}_t(v,t_0)\widehat{\varsigma}_2(v). \tag{13}$$

Equation (13) shows that the rectifying plane of $\widehat{\boldsymbol{\omega}}(v)$ coincides with the tangent plane to the surface $\widehat{\mathcal{M}}$. This means that $\widehat{\boldsymbol{\omega}}(v)$ is a $\mathcal{TL}$ geodesic curve on $\widehat{\mathcal{M}}$. Thus, we gain the following theorem.

Theorem 1. *$\widehat{\boldsymbol{\omega}}(v)$ is an isogeodesic (geodesic for short) on the $\mathcal{TL}$ surface bundle $\widehat{\mathcal{M}}$ if and only if*

$$\left.\begin{array}{l} \mathfrak{x}(v,t_0) = \mathfrak{y}(v,t_0) = 0, \\ \mathfrak{y}_t(v,t_0) \neq 0, \ 0 \le t_0 \le T, \ \ 0 \le v \le L. \end{array}\right\} \tag{14}$$

Any $\mathcal{TL}$ surface fulfilling Equation (14) is an element of this surface bundle. For facilitation and better inspection, the marching-scale functions $\mathfrak{x}(v,t)$ and $\mathfrak{y}(v,t)$ can be displayed in terms of two factors [15]:

$$\begin{aligned} \mathfrak{x}(v,t) &= l(v)\mathfrak{X}(t), \\ \mathfrak{y}(v,t) &= m(v)\mathfrak{Y}(t). \end{aligned} \tag{15}$$

Here, $l(v)$, $m(v)$, $\mathfrak{X}(t)$, and $\mathfrak{Y}(t)$ are C^1 functions that do not identically vanish. Then, from Theorem 1, we derive the following:

Corollary 1. *$\widehat{\omega}(v)$ is a geodesic on the $\mathcal{TL}$ surface bundle $\widehat{\mathcal{M}}$ if and only if*

$$\left.\begin{array}{l} \mathfrak{X}(t_0) = \mathfrak{Y}(t_0) = 0,\ \ l(v) = const. \neq 0,\ m(v) = const. \neq 0, \\ \frac{d\mathfrak{Y}(t_0)}{dt} = const. \neq 0,\ 0 \leq t_0 \leq T,\ \ 0 \leq v \leq L. \end{array}\right\} \tag{16}$$

To achieve the $\mathcal{TL}$ surface bundle $\widehat{\mathcal{M}}$ interpolating $\widehat{\omega}(v)$, we can first determine the marching-scale functions from Equation (16), then employ them in Equations (8) and (9) to derive the parameterization. For suitability in implementation, $\mathfrak{x}(v,t)$ and $\mathfrak{y}(v,t)$ can be, moreover, forced to be in extra limited forms, while still having sufficient degrees of freedom, in order to assign $\widehat{\mathcal{M}}$ with $\widehat{\omega}(v)$ as a shared geodesic $\mathcal{TL}$ curve. Therefore, let us assume that $\mathfrak{x}(v,t)$ and $\mathfrak{y}(v,t)$ can be given in two various configurations, as follows:
(1) If we set

$$\left\{\begin{array}{l} \mathfrak{x}(v,t) = \sum\limits_{k=1}^{p} a_{1k} l(v)^k \mathfrak{X}(t)^k, \\ \mathfrak{y}(v,t) = \sum\limits_{k=1}^{p} b_{1k} m(v)^k \mathfrak{Y}(t)^k, \end{array}\right. \tag{17}$$

then we can naturally indicate the sufficient condition for $\widehat{\omega}(v)$ being $\mathcal{TL}$ geodesic curves on $\widehat{\mathcal{M}}$ as

$$\left\{\begin{array}{c} \mathfrak{X}(t_0) = \mathfrak{Y}(t_0) = 0, \\ b_{11} \neq 0,\ m(v) \neq 0, \text{and } \frac{d\mathfrak{X}(t_0)}{dt} = const. \neq 0, \end{array}\right. \tag{18}$$

where $l(v)$, $m(v)$, $\mathfrak{X}(t), \mathfrak{Y}(t) \in C^1$, a_{ij}, $b_{ij} \in \mathbb{R}$ $(i = 1,2; j = 1,2,...,p)$ and $l(v)$ and $m(v)$ are not identically zero.
(2) If we set

$$\left\{\begin{array}{l} \mathfrak{x}(v,t) = f(\sum\limits_{k=1}^{p} a_{1k} l^k(v)\mathfrak{X}^k(t)), \\ \mathfrak{y}(v,t) = g(\sum\limits_{k=1}^{p} b_{1k} m^k(v)\mathfrak{Y}^k(t)), \end{array}\right. \tag{19}$$

then

$$\left\{\begin{array}{c} \mathfrak{X}(t_0) = \mathfrak{Y}(t_0) = f(0) = g(0) = 0, \\ b_{11} \neq 0,\ \frac{d\mathfrak{Y}(t_0)}{dt} = const \neq 0,\ m(v) \neq 0,\ g'(0) \neq 0, \end{array}\right. \tag{20}$$

where $l(v)$, $m(v)$, $\mathfrak{X}(t), \mathfrak{Y}(t) \in C^1$, a_{ij}, $b_{ij} \in \mathbb{R}$ $(i = 1,2; j = 1,2,\ldots,p)$ and $l(v)$ and $m(v)$ are not identically zero. As there are no constraints associated with the curves specified in Equations (16), (18) or (20), the $\mathcal{TL}$ surface bundle $\widehat{\mathcal{M}}$ with $\widehat{\omega}(v)$ as joint geodesic $\mathcal{TL}$ curve can be derived by choosing appropriate marching-scale functions. We use $\{\widehat{\mathcal{M}}, \mathcal{M}\}$ to denote the $\mathcal{TLSC}$ with $\mathcal{BC}$ $\{\widehat{\omega}(v), \omega(v)\}$ as common geodesic curves.

Example 1. *Consider the $\mathcal{TL}$ circular helix*

$$\omega(v) = (\sqrt{3}\cosh v, \sqrt{2}v, \sqrt{3}\sinh v),\ -2 \leq s \leq 2.$$

Then

$$\left.\begin{array}{r}\varsigma_1(v) = (\sqrt{3}\sinh v, \sqrt{2}, \sqrt{3}\cosh v),\\ \varsigma_2(v) = (\cosh v, 0, \sinh v),\\ \varsigma_3(v) = (\sqrt{2}\sinh v, \sqrt{3}, -\sqrt{2}\cosh v).\end{array}\right\}$$

The$\mathcal{TL}$ surface bundle $\mathcal{M}$ with $\boldsymbol{\omega}(v)$ as joint $\mathcal{TL}$ geodesic curve is

$$\mathcal{M} \quad : \quad \mathfrak{r}(v,t) = (\sqrt{3}\cosh v, \sqrt{2}v, \sqrt{3}\sinh v) + (\mathfrak{x}(v,t), 0, \mathfrak{y}(v,t)) \times \begin{pmatrix} \sqrt{3}\sinh v & \sqrt{2} & \sqrt{3}\cosh v \\ \cosh v & 0 & \sinh v \\ \sqrt{2}\sinh v & \sqrt{3} & -\sqrt{2}\cosh v \end{pmatrix},$$

where $-1 \leq t \leq 1$ *and* $-2 \leq v \leq 2$*. If* $f = -2\sqrt{3}$ *in Equation (5), then*

$$\widehat{\boldsymbol{\omega}}(v) := \boldsymbol{\omega}(v) - 2\sqrt{3}\varsigma_2(v) = (-\sqrt{3}\cosh v, \sqrt{2}v, -\sqrt{3}\sinh v),$$

and

$$\left.\begin{array}{r}\widehat{\varsigma}_1(v) = (-\sqrt{3}\sinh v, \sqrt{2}, -\sqrt{3}\cosh v),\\ \widehat{\varsigma}_2(v) = (-\cosh v, 0, -\sinh v),\\ \widehat{\varsigma}_3(v) = (-\sqrt{2}\sinh v, \sqrt{3}, -\sqrt{2}\cosh v).\end{array}\right\}$$

The $\mathcal{TL}$ surface bundle $\widehat{\mathcal{M}}$ with $\widehat{\boldsymbol{\omega}}(v)$ as joint $\mathcal{TL}$ geodesic curve is

$$\widehat{\mathcal{M}} \quad : \quad \widehat{\mathfrak{r}}(v,t) = (-\sqrt{3}\cosh v, \sqrt{2}v, -\sqrt{3}\sinh v) + (\mathfrak{x}(v,t), 0, \mathfrak{y}(v,t)) \times \begin{pmatrix} -\sqrt{3}\sinh v & \sqrt{2} & -\sqrt{3}\cosh v \\ -\cosh v & 0 & -\sinh v \\ -\sqrt{2}\sinh v & \sqrt{3} & -\sqrt{2}\cosh v \end{pmatrix}.$$

Choosing $\mathfrak{x}(v,t) = \sin t$*,* $\mathfrak{y}(v,t) = 1 - \cos t$*, and* $t_0 = 0$*, then Equation (16) is satisfied and the obtained* $\{\mathcal{M}, \widehat{\mathcal{M}}\}$ *is shown in Figure 1, where the blue curve symbolizes* $\widehat{\boldsymbol{\omega}}(v)$ *on* $\widehat{\mathfrak{M}}$*, and the green curve is* $\boldsymbol{\omega}(v)$ *on* $\mathfrak{M}$*.*

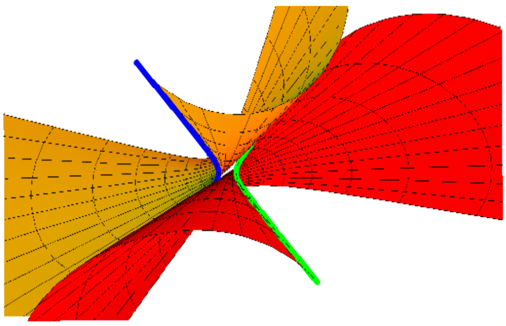

Figure 1. $\{\widehat{\mathfrak{M}}, \mathfrak{M}\}$ with $\mathfrak{x}(v,t) = \sin t$, $\mathfrak{y}(v,t) = 1 - \cos t$, and $t_0 = 0$.

Example 2. *Let* $\boldsymbol{\omega}(v)$ *be a $\mathcal{TL}$ helix defined by*

$$\boldsymbol{\omega}(v) = (\sqrt{2}\cos v, \sqrt{2}\sin v, \sqrt{3}v),\ 0 \leq v \leq 2\pi.$$

Then

$$\left.\begin{array}{r}\varsigma_1(v) = (-\sqrt{2}\sin v, \sqrt{2}\cos v, \sqrt{3}),\\ \varsigma_2(v) = (-\cos v, -\sin v, 0),\\ \varsigma_3(v) = (\sqrt{3}\sin v, -\sqrt{3}\cos v, -\sqrt{2}).\end{array}\right\}$$

The $\mathcal{TL}$ surface bundle $\mathcal{M}$ with $\boldsymbol{\omega}(v)$ as joint $\mathcal{TL}$ geodesic curve is given by

$$\mathcal{M} \quad : \quad \mathfrak{r}(s,t) = (\sqrt{2}\cos v, \sqrt{2}\sin v, \sqrt{3}v) + (\mathfrak{x}(v,t), 0, \mathfrak{y}(v,t)) \times \begin{pmatrix} -\sqrt{2}\sin v & \sqrt{2}\cos v & \sqrt{3} \\ -\cos v & -\sin v & 0 \\ \sqrt{3}\sin v & -\sqrt{3}\cos v & -\sqrt{2} \end{pmatrix},$$

where $-1 \leq t \leq 1$ and $0 \leq v \leq 2\pi$. If $f = 2\sqrt{2}$ in Equation (5), then

$$\widehat{\boldsymbol{\omega}}(v) := \boldsymbol{\omega}(v) + 2\sqrt{2}\varsigma_2(v) = (-\sqrt{2}\cos v, -\sqrt{2}\sin v, \sqrt{3}v),$$

and

$$\left.\begin{array}{r} \widehat{\varsigma}_1(v) = (\sqrt{2}\sin v, -\sqrt{2}\cos v, \sqrt{3}), \\ \widehat{\varsigma}_2(v) = (\cos v, \sin v, 0), \\ \widehat{\varsigma}_3(v) = (-\sqrt{3}\sin v, \sqrt{3}\cos v, -\sqrt{2}). \end{array}\right\}$$

The $\mathcal{TL}$ surface bundle $\widehat{\mathcal{M}}$ with $\widehat{\boldsymbol{\omega}}(v)$ as joint $\mathcal{TL}$ geodesic curve is

$$\widehat{\mathcal{M}} \quad : \quad \widehat{\mathfrak{r}}(v,t) = -\sqrt{2}\cos v, -\sqrt{2}\sin v, \sqrt{3}v) + (\mathfrak{x}(v,t), 0, \mathfrak{y}(v,t)) \times \begin{pmatrix} \sqrt{2}\sin v & -\sqrt{2}\cos v & \sqrt{3} \\ \cos v & \sin v & 0 \\ \sqrt{3}\sin v & \sqrt{3}\cos v & -\sqrt{2} \end{pmatrix}.$$

(1) Taking

$$\left.\begin{array}{l} \mathfrak{x}(v,t) = (1+\sin t) + \sum_{k=2}^{4} a_{1k}(1+\sin t)^k, \\ \mathfrak{y}(v,t) = (1-\cos t) + \sum_{k=2}^{4} b_{1k}(1-\cos t)^k, \end{array}\right\} \tag{a}$$

where $-\pi/4 \leq t \leq \pi/4$ and $0 \leq v \leq 2\pi$, $t_0 = 0$, and a_{1k}, $b_{1k} \in \mathbb{R}$, then Equation (18) is satisfied. If $a_{1k} = b_{1k} = 1$, then the resulting $\{\mathcal{M}, \widehat{\mathcal{M}}\}$ is shown in Figure 2, where the blue curve symbolizes $\widehat{\boldsymbol{\omega}}(v)$ on $\widehat{\mathcal{M}}$, and the green curve is $\boldsymbol{\omega}(v)$ on $\mathcal{M}$.

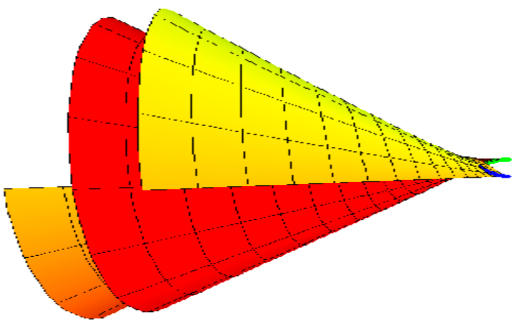

Figure 2. $\{\widehat{\mathcal{M}}, \mathcal{M}\}$ with $\mathfrak{x}(v,t)$, and $\mathfrak{y}(v,t)$ as in Equation (a).

(2) Selecting

$$\mathfrak{x}(v,t) = \sin t + \sum_{k=2}^{4} a_{1k}\sin^k t, \; \mathfrak{y}(v,t) = 1 - \cos t + \sum_{k=1}^{4} b_{1k}(1-\cos t)^k, \tag{b}$$

where $-\pi/2 \leq t \leq \pi/2$, $0 \leq v \leq 2\pi$, $t_0 = 0$, and a_{1k}, $b_{1k} \in \mathbb{R}$; then, Equation (20) is satisfied. For $a_{1k} = b_{1k} = 1$, the obtained $\{\mathcal{M}, \widehat{\mathcal{M}}\}$ is plotted in Figure 3, where the blue curve symbolizes $\widehat{\boldsymbol{\omega}}(v)$ on $\widehat{\mathcal{M}}$, and the green curve is $\boldsymbol{\omega}(v)$ on $\mathcal{M}$.

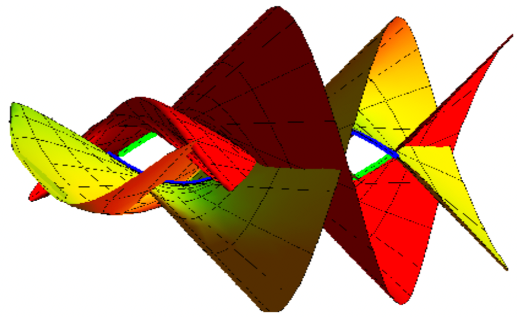

Figure 3. $\{\widehat{\mathcal{M}}, \mathcal{M}\}$ with $\mathfrak{x}(v,t)$, and $\mathfrak{y}(v,t)$, as in Equation (b).

Note that we could continue with this series of $\mathcal{TL}$ surfaces through selecting different collections of characteristic curves or numbers of curves to interpolate.

Ruled $\mathcal{TLSC}$ with Joint $\mathcal{TL}$ Geodesic $\mathcal{BC}$

Ruled surfaces play an important role in various types of design, architecture, manufacturing, art and sculpture. They can be created in a variety of ways, which is a topic that has been the subject of a lot of discussion in mathematics and engineering journals. In geometric modeling, a ruled surface is a special surface created through the continuous motion of a line (ruling) on a curve, which acts as the base curve.

Let us consider that $\widehat{\omega}(v)$ is a unit speed $\mathcal{TL}$ curve. Assume that $\widehat{\mathfrak{r}}(s,t)$ is a $\mathcal{TL}$ ruled surface with the base curve $\widehat{\omega}(v)$, and $\widehat{\omega}(v)$ is also an isoparametric $\mathcal{TL}$ curve of $\widehat{\mathfrak{r}}(v,t)$. Then, there exists t_0 such that $\widehat{\mathfrak{r}}(v,t_0) = \widehat{\omega}(v)$. It follows that

$$\widehat{\mathcal{M}} : \widehat{\mathfrak{r}}(v,t) - \widehat{\mathfrak{r}}(v,t_0) = (t-t_0)\widehat{e}(v), \text{ with } 0 \leq v \leq L,\ t,\ t_0 \in [0,T],$$

where $\widehat{e}(v)$ is a $\mathcal{TL}$ unit vector along the rulings. According to Equation (9), we have

$$(t-t_0)\widehat{e}(v) = \mathfrak{x}(v,t)\widehat{\varsigma}_1(v) + \mathfrak{y}(v,t)\widehat{\varsigma}_3(v),\ 0 \leq v \leq L, \text{ with } t,\ t_0 \in [0,T], \tag{21}$$

which is a system of two equations with two unknown functions $\mathfrak{x}(v,t)$ and $\mathfrak{y}(v,t)$. To solve the functions $\mathfrak{x}(v,t)$ and $\mathfrak{y}(v,t)$, we have

$$\begin{aligned} \mathfrak{x}(v,t) &= -(t-t_0)\langle \widehat{e}, \widehat{\varsigma}_1 \rangle = -(t-t_0)\det(\widehat{e}, \widehat{\varsigma}_2, \widehat{\varsigma}_3), \\ \mathfrak{y}(v,t) &= (t-t_0)\langle \widehat{e}, \widehat{\varsigma}_3 \rangle = (t-t_0)\det(\widehat{e}, \widehat{\varsigma}_1, \widehat{\varsigma}_2). \end{aligned} \tag{22}$$

Equation (22) precisely provides the necessary and sufficient conditions for $\widehat{\mathcal{M}}$ to be a $\mathcal{TL}$ ruled surface. In view of Theorem 1, if the curve $\widehat{\omega}(v)$ is also a $\mathcal{TL}$ geodesic curve on $\widehat{\mathcal{M}}$, then $\det(\widehat{e}, \widehat{\varsigma}_1, \widehat{\varsigma}_2) \neq 0$. Thus, at any point on the $\mathcal{TL}$ curve $\widehat{\omega}(v)$, the ruling direction $\widehat{e}(v) \in Sp\{\widehat{\varsigma}_1, \widehat{\varsigma}_2\}$. Furthermore, the vectors $\widehat{e}(v)$ and $\widehat{\varsigma}_1(v)$ must not be identical. This leads to

$$\widehat{e}(v) = \gamma(v)\widehat{\varsigma}_1(v) + \beta(v)\widehat{\varsigma}_3(v),\ 0 \leq v \leq L, \tag{23}$$

for some real functions $\beta(v) \neq 0$ and $\gamma(v)$. Then

$$\widehat{\mathcal{M}} : \widehat{\mathfrak{r}}(v,t) = \widehat{\omega}(v) + t(\gamma(s)\widehat{\varsigma}_1(v) + \beta(v)\widehat{\varsigma}_3(v)),\ 0 \leq v \leq L,\ 0 \leq t \leq T, \tag{24}$$

where $\gamma(v)$ and $\beta(v) \neq 0$. However, the $\mathcal{SL}$ normal vector to $\widehat{\mathcal{M}}$ along the curve $\widehat{\omega}(v)$ is

$$\widehat{\mathcal{N}}(v,t_0) = \beta(v)\widehat{\varsigma}_2(v). \tag{25}$$

Equation (25) shows that $\widehat{\omega}(v)$ is a $\mathcal{TL}$ geodesic curve on $\widehat{\mathcal{M}}$. Thus, the following theorem can be stated.

Theorem 2. *The ruled $\mathcal{TLSC}$ $\{\mathcal{M}, \widehat{\mathcal{M}}\}$ interpolates the $\mathcal{TLBC}$ $\{\boldsymbol{\omega}(v), \widehat{\boldsymbol{\omega}}(v)\}$ as joint geodesic $\mathcal{TL}$ curves if there exist a parameter $t_0 \in [0, T]$ and the functions $\gamma(v), \beta(v) \neq 0$ such that $\widehat{\mathcal{M}}$ and $\mathcal{M}$ satisfy Equation (25), and*

$$\mathcal{M} : \mathfrak{r}(v, t) = \boldsymbol{\omega}(v) + t(\gamma(v)\varsigma_1(s) + \beta(v)\varsigma_3(v)),\ 0 \leq v \leq L,\ 0 \leq t \leq T. \tag{26}$$

It must be pointed out that, in Equations (25) and (26), there exist two geodesic $\mathcal{TL}$ curves crossing through every point on the curves $\widehat{\boldsymbol{\omega}}(v)(\boldsymbol{\omega}(v))$, where one is $\widehat{\boldsymbol{\omega}}$ itself and the other is a geodesic $\mathcal{TL}$ line in the orientation $\widehat{e}(v)$, as given in Equation (23). Every constituent of the isoparametric ruled $\mathcal{TL}$ surface bundle with the joint $\mathcal{TL}$ geodesic $\widehat{\boldsymbol{\omega}}$ is defined by two set functions, $\gamma(v)$ and $\beta(v) \neq 0$.

Example 3. *Considering Example 1, we have*
If $\gamma(v) = 0$, $\beta(v) = -1$, the ruled $\mathcal{TLSC}$ $\{\mathcal{M}, \widehat{\mathcal{M}}\}$ with $\mathcal{TLBC}$ $\{\boldsymbol{\omega}(v), \widehat{\boldsymbol{\omega}}(v)\}$ is

$$\begin{cases} \mathcal{M} : \mathfrak{r}(v, t) = (\sqrt{3}\cosh v - \sqrt{2}t\sinh v, \sqrt{2}v + \sqrt{3}t, \sqrt{3}\sinh v - \sqrt{2}t\cosh v), \\ \widehat{\mathcal{M}} : \widehat{\mathfrak{r}}(v, t) = (-\sqrt{3}\cosh v - \sqrt{2}t\sinh v, \sqrt{2}v + \sqrt{3}t, -\sqrt{3}\sinh v - \sqrt{2}t\cosh v), \end{cases}$$

where $-10 \leq t \leq 10$, $-1.5 \leq v \leq 1.5$. The surface is shown in Figure 4, where the blue curve symbolizes $\widehat{\boldsymbol{\omega}}(v)$ on $\widehat{\mathcal{M}}$, and the green curve is $\boldsymbol{\omega}(v)$ on $\mathcal{M}$.

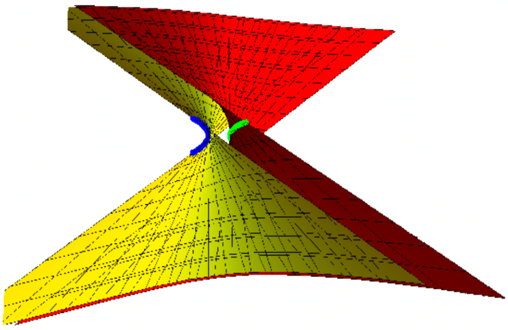

Figure 4. $\{\mathcal{M}, \widehat{\mathcal{M}}\}$ with $\gamma(v) = 0$, $\beta(v) = -1$.

Example 4. *Considering Example 2, we have:*
(1) If $\gamma(v) = 0$, $\beta(v) = -1$, the ruled $\mathcal{TLSC}$ $\{\mathcal{M}, \widehat{\mathcal{M}}\}$ with $\mathcal{TLBC}$ $\{\boldsymbol{\omega}(v), \widehat{\boldsymbol{\omega}}(v)\}$ is:

$$\begin{cases} \mathcal{M} : \mathfrak{r}(v, t) = (\sqrt{3}\cos v - \sqrt{3}t\sin v, \sqrt{2}\sin v - \sqrt{3}t\cos v, \sqrt{3}v - \sqrt{2}t), \\ \widehat{\mathcal{M}} : \widehat{\mathfrak{r}}(v, t) = (-\sqrt{3}\cos v - \sqrt{3}t\sin v, -\sqrt{2}\sin v - \sqrt{3}t\cos v, \sqrt{3}v - \sqrt{2}t), \end{cases}$$

where $0 \leq t \leq 3$, $0 \leq v \leq 2\pi$. The surface is shown in Figure 5, where the blue curve is $\widehat{\boldsymbol{\omega}}(v)$ on $\widehat{\mathcal{M}}$, and the green curve is $\boldsymbol{\omega}(v)$ on $\mathcal{M}$.

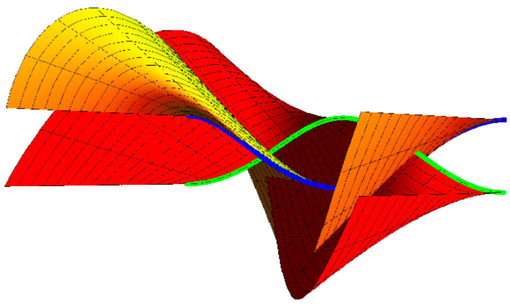

Figure 5. $\{\mathcal{M}, \widehat{\mathcal{M}}\}$ with $\gamma(v) = 0$, $\beta(v) = -1$.

(2) If $\gamma(v) = \beta(v) = 1$, the ruled $\mathcal{TLSC}$ $\{\mathcal{M}, \widehat{\mathcal{M}}\}$ with $\mathcal{TLBC}$ $\{\boldsymbol{\omega}(v), \widehat{\boldsymbol{\omega}}(v)\}$ is

$$\begin{cases} \mathcal{M}:\mathfrak{r}(v,t)=(\sqrt{2}\cos v+t(\sqrt{3}-\sqrt{2})\sin v,\sqrt{2}\sin v-t(\sqrt{3}-\sqrt{2})\cos v,t(\sqrt{3}-\sqrt{2})), \\ \widehat{\mathcal{M}}:\widehat{\mathfrak{r}}(v,t)=(-\sqrt{2}\cos v+t(\sqrt{3}+\sqrt{2})\sin v,-\sqrt{2}\sin v+t(\sqrt{3}-\sqrt{2})\cos v,t(\sqrt{3}-\sqrt{2})), \end{cases}$$

where $-3\leq t\leq 3$, $0\leq v\leq 2\pi$. *The surface is shown in Figure 6, where the blue curve symbolizes* $\widehat{\boldsymbol{\omega}}(v)$ *on* $\widehat{\mathcal{M}}$, *and the green curve is* $\boldsymbol{\omega}(v)$ *on* $\mathcal{M}$.

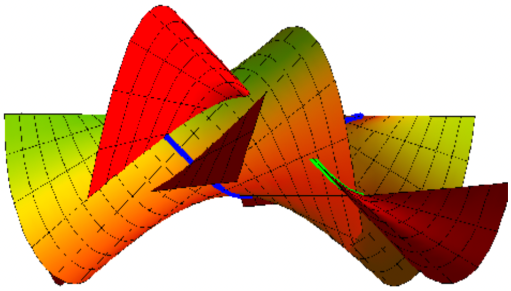

Figure 6. $\{\mathcal{M},\widehat{\mathcal{M}}\}$ with $\gamma(v)=\beta(v)=1$.

4. Conclusions

In this paper, we established a theory related to a $\mathcal{TLSC}$ with $\mathcal{TLBC}$ as a pair of geodesic curves in Minkowski 3-space $\mathcal{E}_1^3$. Subsequently, the outcomes for the ruled $\mathcal{TLSC}$ with $\mathcal{TLBC}$ as geodesic curves were also addressed. More specifically, this research seeks to investigate the geometric analysis of pairs of timelike surfaces through the utilization of the timelike Bertrand pair. For validation of our results, some models were specified in order to construct the $\mathcal{TLSC}$ and ruled $\mathcal{TLSC}$ using joint $\mathcal{TLBC}$. We focused on the kind of ruled surfaces because their geometry is necessary to study kinematics, spatial mechanisms, surface design, robotic research and manufacturing technology [46–48]. This study has a deeper and more meaningful approach when it depends on the curvature theory to recalculate the robot's motion curve [49]. In future work, we will attempt to integrate the singularity and submanifold theories defined in [50–52], among others, with the consequences of this work. Hopefully, these consequences will be helpful for physicists, especially those concerned with general relativity theory.

Funding: Princess Nourah bint Abdulrahman University Researchers Supporting Project number (PNURSP2024R27), Princess Nourah bint Abdulrahman University, Riyadh, Saudi Arabia.

Data Availability Statement: All the necessary data are contained within the article.

Acknowledgments: The author expresses her sincere gratitude to Rashad A. Abdel-Baky for his productive consultations. The author expresses her gratitude to Princess Nourah bint Abdulrahman University Researchers Supporting Project number (PNURSP2024R27), Princess Nourah bint Abdulrahman University, Riyadh, Saudi Arabia. I thank the anonymous reviewers for their careful reading of the manuscript and their many insightful comments and suggestions.

Conflicts of Interest: The author declares no conflicts of interest.

References

1. Spivak, M.A. *Comprehensive Introduction to Differential Geometry*, 2nd ed.; Publish or Perish: Houston, TX, USA, 1979.
2. Do Carmo, M.P. *Differential Geometry of Curves and Surfaces*; Prentice-Hall: Englewood Cliffs, NJ, USA, 1976.
3. O'Neil, B. *Semi-Riemannian Geometry, with Applications to Relativity*; Academic Press: New York, NY, USA, 1983.
4. Walfare, J. Curves and Surfaces in Minkowski Space. Ph.D. Thesis, Faculty of Science, K.U. Leuven, Leuven, Belgium, 1995.
5. Ravani, B.; Ku, T.S. Bertrand offsets of ruled and developable surfaces. *Comput.-Aided Des.* **1991**, *23*, 145–152. [CrossRef]
6. Sprott, K.S.; Ravani, B. Cylindrical milling of ruled surfaces. *Int. J. Adv. Manuf. Technol.* **2008**, *38*, 649–656. [CrossRef]
7. Brond, R.; Jeulin, D.; Gateau, P.; Jarrin, J.; Serpe, G. Estimation of the transport properties of polymer composites by geodesic propagation. *J. Microsc.* **1994**, *176*, 167–177. [CrossRef]
8. Bryson, S. Virtual spacetime: An environment for the visualization of curved spacetimes via geodesic flows. In Proceedings of the Proceedings Visualization '92, Boston, MA, USA, 19–23 October 1992; pp. 291–298.
9. Haw, R.J.; Munchmeyer, R.C. Geodesic curves on patched polynomial surfaces. *Comput. Graph. Forum* **1983**, *2*, 225–232. [CrossRef]

10. Agarwal, K.; Har-Peled, S.; Sharir, M.; Varadarajan, K.R. Approximating shortest paths on a convex polytope in three dimensions. *J. ACM* **1997**, *44*, 567–584. [CrossRef]
11. Har-Peled, S. Approximate shortest-path and geodesic diameter on convex polytopes in three dimensions. *Discret. Comput. Geom.* **1999**, *21*, 217–231. [CrossRef]
12. Haw, R.J. An application of geodesic curves to sail design. *Comput. Graph. Forum* **1985**, *4*, 137–139. [CrossRef]
13. Goldenberg, R.; Kimmel, R.; Rivlin, E.; Rudzsky, M. Fast geodesic active contours. *IEEE Trans. Image Process* **2001**, *10*, 1467–1475. [CrossRef] [PubMed]
14. Novotni, M.; Klein, R. Computing geodesic paths on triangular meshes. In Proceedings of the 17th Brazilian Symposium on Computer Graphics and Image Processing, Curitiba, Brazil, 20 October 2004; pp. 341–347.
15. Wang, G.J.; Tang, K.; Tai, C.L. Parametric representation of a surface bundle with a common spatial geodesic. *Comput.-Aided Des.* **2004**, *36*, 447–459. [CrossRef]
16. Zhao, H.Y.; Wang, G.J. A new method for designing a developable surface utilizing the surface bundle through a given curve. *Prog. Nat. Sci.* **2008**, *18*, 105–110. [CrossRef]
17. Li, C.Y.; Wang, R.H.; Zhu, C.G. An approach for designing a developable surface through a given line of curvature. *Comput.-Aided Des.* **2013**, *45*, 621–627. [CrossRef]
18. Liu, Y.; Wang, G.J. Designing developable surface bundle through given curve as its common asymptotic curve. *J. Zhejiang Univ.* **2013**, *47*, 1246–1252.
19. Atalay, G.S.; Kasap, E. Surfaces family with common Smarandache geodesic curve. *J. Sci. Arts* **2017**, *4*, 651–664.
20. Abdel-Baky, R.A.; Alluhaib, N. Surfaces family with a common geodesic curve in Euclidean 3-Space $\mathbb{E}^3$. *Int. J. Math. Anal.* **2019**, *13*, 433–447. [CrossRef]
21. Abdel-Baky, R.A. Timelike surfaces with a common asymptotic curve in Minkowski 3-Space $\mathbb{E}^3_1$. *Riv. Mat. Univ. Parma* **2017**, *8*, 379–395.
22. Ergün, E.; Bayram, E.; Kasap, E. Surface bundle with a common line of curvature in Minkowski 3-space. *Acta Math. Sin.* **2014**, *30*, 2103–2118. [CrossRef]
23. Alluhaib, N.; Abdel-Baky, R.A. A surface family with a common asymptotic null curve in Minkowski 3-space $\mathbb{E}^3_1$. *Math. Probl. Eng.* **2021**, *2021*, 3901527.
24. Atalay, G.S.; Kasap, E. Surfaces family with common null asymptotic. *Appl. Math. Comput.* **2015**, *260*, 135–139. [CrossRef]
25. Atalay, G.S. Surfaces family with a common Mannheim geodesic curve. *J. Appl. Math. Comput.* **2018**, *2*, 155–165.
26. Jiang, X.; Jiang, P.; Meng, J.; Wang, K. Surface bundle couple interpolating Bertrand couple as common asymptotic curves in Galilean space $\mathbb{G}_3$. *Int. J. Geom. Methods Mod. Phys.* **2021**, *18*, 2150114 [CrossRef]
27. Almoneef, A.A.; Abdel-Baky, R.A. Surface family couple with Bertrand couple as common geodesic curves in Galilean 3-space $\mathbb{G}_3$. *Mathematics* **2023**, *11*, 2391. [CrossRef]
28. Matsuda, H.; Yorozu, S. Notes on Bertrand curves. *Yokohama Math. J.* **2003**, *50*, 41–58.
29. Almoneef, A.A.; Abdel-Baky, R.A. Surface family couple with Bertrand couple as mutual geodesic curves in Euclidean 3-space. *AIMS Math.* **2023**, *8*, 20546–20560. [CrossRef]
30. Al-Jedani, A.; Abdel-Baky, R.A. A surface family with a mutual geodesic curve in Galilean 3-space $\mathbb{G}_3$. *Mathematics* **2023**, *11*, 2971. [CrossRef]
31. Papaioannou, S.G.; Kiritsis, D. An application of Bertrand curves and surface to CAD/CAM. *Comput.-Aided Des.* **1985**, *17*, 348–352. [CrossRef]
32. Görgülü, E.; Ozdamar, E. A generalizations of the Bertrand curves as general inclined curves in E n. *Commun. Fac. Sci. Uni. Ankara. Ser. A1* **1986**, *35*, 53–60. [CrossRef]
33. Izumiya, S.; Takeuchi, N. Generic properties of helices and Bertrand curves. *J. Geom.* **2002**, *74*, 97–109. [CrossRef]
34. Tanriöver, N. Some properties of Bertrand curves in Lorentzian n-space $\mathbb{L}^n$. *Int. J. Geom. Methods Mod. Phys.* **2016**, *13*, 1650064. [CrossRef]
35. Whittemore, J.K. Bertrand curves and helices. *Duke Math. J.* **1940**, *6*, 235–245. [CrossRef]
36. Kazaz, M.; Uğurlu, H.H. Bertrand Partner D-Curves in the minkowski3-space E3-1. *Math. Sci. Appl. E-Notes* **2014**, *2*, 68–82.
37. Aksoyak, F.K.; Gök, I.S.M.A.I.L.; Ilarslan, K. Generalized null Bertrand curves in Minkowski space-time. *Ann. Alexandru Ioan Cuza Univ. Math.* **2014**, *60*, 489–502. [CrossRef]
38. Magid, M.A. Timelike surfaces in Lorentz 3-space with prescribed mean curvature and Gauss map. *Hokkaido Math. J.* **1991**, *20*, 447–464. [CrossRef]
39. Önder, M.; Uğurlu, H.H. Frenet frames and invariants of timelike ruled surfaces. *Ain Shams Eng. J.* **2013**, *4*, 507–513. [CrossRef]
40. Babaarslan, M.; Munteanu, M.I. Time-like loxodromes on rotational surfaces in Minkowski 3-space. *Ann. Alexandru Ioan Cuza Univ.-Math.* **2015**, *61*, 471–484.
41. Alluhaibi, N.; Abdel-Baky, R.A. Kinematic Geometry of Timelike Ruled Surfaces in Minkowski 3-Space $\mathbb{E}^3_1$. *Symmetry* **2022**, *14*, 749. [CrossRef]
42. Babaarslan, M.; Kayacik, M. Time-like loxodromes on helicoidal surfaces in Minkowski 3-space. *Filomat* **2017**, *31*, 4405–4414. [CrossRef]
43. Li, Y.; Mofarreh, F.; Abdel-Baky, R.A. Timelike Circular Surfaces and Singularities in Minkowski 3-Space. *Symmetry* **2022**, *14*, 1914. [CrossRef]

44. Wang, Y.; Yang, L.; Li, P.; Chang, Y. Singularities of Osculating Developable Surfaces of Timelike Surfaces along Curves. *Symmetry* **2022**, *14*, 2251. [CrossRef]
45. Gür, M.S. Geometric properties of timelike surfaces in Lorentz-Minkowski 3-space. *Filomat* **2023**, *37*, 5735–5749. [CrossRef]
46. Yapar, Z.; Sa, Y. On the geometry of closed timelike ruled surfaces in dual Lorentzian space. *Int. J. Appl. Math.* **2016**, *29*, 7–18. [CrossRef]
47. Yapar, Z.; Sagiroglu, Y. On a motion of a line along two closed ruled surfaces. *Int. J. Math. Anal.* **2015**, *9*, 1877–1887. [CrossRef]
48. Atalay, G.Ş.; Kasap, E. Developed Motion of Robot End-Effector of Timelike Ruled Surfaces With Spacelike Rulings (The First Case). *Hagia Sophia J. Geom.* **2020**, *2*, 9–21.
49. Güler, F.; Kasap, E. A path planning method for robot end effector motion using the curvature theory of the ruled surfaces. *Int. J. Geom. Methods Mod. Phys.* **2018**, *15*, 1850048. [CrossRef]
50. Li, Y.L.; Zhu, Y.S.; Sun, Q.Y. Singularities and dualities of pedal curves in pseudo-hyperbolic and de Sitter space. *Int. J. Geom. Methods Mod. Phys.* **2021**, *18*, 2150008. [CrossRef]
51. Li, Y.L.; Nazra, S.; Abdel-Baky, R.A.; Singularities properties of timelike sweeping surface in Minkowski 3-Space. *Symmetry* **2022**, *14*, 1996. [CrossRef]
52. Li, Y.L.; Chen, Z.; Nazra, S.; Abdel-Baky, R.A. Singularities for timelike developable surfaces in Minkowski 3-Space. *Symmetry* **2023**, *15*, 277. [CrossRef]